

## **Reflection Effect in Close Binaries. V. Effects of Reflection on Spectral Line Formation**

A. Peraiah and M. Srinivasa Rao *Indian Institute of Astrophysics, Bangalore 560034*

Received 1983 February 9; accepted 1983 July 6

**Abstract.** The effects of reflection on the formation of spectral lines is investigated. We have assumed a purely scattering atmosphere and studied how the equivalent widths change due to irradiation from the secondary. Generally, the flux in the lines is increased at all frequency points, the cores of the lines receiving more flux than the wings. Moreover, the proximity of the secondary component changes the equivalent widths considerably. The further away the secondary is from the primary the higher are the equivalent widths.

*Key words:* reflection effect—spectral line formation

### **1. Introduction**

We have investigated so far (Peraiah 1982: Paper 1; Peraiah 1983a: Paper 2; Peraiah 1983b: Paper 3; Peraiah & Rao, 1983: Paper 4), how the irradiation from the secondary component changes the radiation field in the atmosphere of the primary. This has been done assuming a purely scattering atmosphere in a monochromatic situation. This also helps in proper understanding of the observed total light that is emitted by the system. Napier & Ovenden (1970) tried to explain by means of reflection effect, the correlation between the velocity amplitudes of individual absorption lines and their wavelengths observed in 57 Cygni. However, they could not succeed in this, because of the fact that they did not use a detailed calculation of the radiation field modified by the incidence of the external radiation. There is another important observational aspect in close binaries that must be understood clearly—the change in the equivalent widths of the lines between eclipses. The spectral lines in 12 Lacertae undergo a periodic variation in width, the lines being wide and diffuse at periastron and sharper and narrower at apastron (Young 1922). There are several explanations put forward for explaining this phenomenon. However, the fact that the lines become wide and diffuse at periastron point, indicates that mutually reflected radiation increases the flux in the lines because of the proximity of the two components. Therefore, we shall study in the present paper how reflection affects the spectral lines. We shall assume a purely scattering medium.

## 2. Computational procedure and discussion of the results

The procedure to calculate the lines is similar to that used to calculate the radiation in the scattering medium due to electrons. The radiative transfer equation which is employed in calculating the source function due to self-radiation is written as (see Grant & Peraiah 1972),

$$\mu \frac{\partial I(x, \mu, r)}{\partial r} + \frac{1 - \mu^2}{r} \frac{\partial I(x, \mu, r)}{\partial \mu} = K_L(r) [\beta + \phi(x)] [S_s(x, r) - I(x, \mu, r)]. \quad (1)$$

Here,  $I(x, \mu, r)$  is the specific intensity of the ray making an angle  $\cos^{-1} \mu$  with the radius vector  $r$ .  $x$  is the standardised frequency given by

$$x = (v - v_0) / \Delta_s$$

where  $\Delta_s$  is a standard frequency interval.  $S_s(x, r)$  is the source function at  $r$  for the frequency  $x$ . We have considered a Doppler profile for  $\phi(x)$ .  $K_L(x)$  is the absorption coefficient at the centre of the line per unit interval of  $\Delta_s$ .  $\beta$  is the ratio of the opacity in the continuum to that in the line per unit frequency interval. The procedure of solving the equation is described in Grant and Peraiah (1972). We have set  $\beta$  equal to zero. We have assumed a purely scattering medium due to electrons and used Thomson scattering coefficient in calculating the optical depth. We have assumed that the continuum radiation is supplied by the star. We specify the quantity  $I(\tau = T, \mu, x)$  where  $T$  is the maximum optical depth (measured from outside towards the centre of the star).

The calculation of the source function due to irradiation  $S_I$ , is described in Paper 4. The geometry is described in Fig. 1.  $O$  is the centre of the component whose atmosphere is facing the secondary with its centre at  $O'$ . The atmosphere of  $O$  is divided into several shells of equal geometrical thickness. We consider rays parallel to the line of sight. Each ray is drawn as tangent to the shell boundary where this boundary meets the  $OO'$  axis. This means that we set the orbital plane of the binary to be perpendicular to the line of sight. We compute the total source functions at points such as  $P$  where the rays intersect

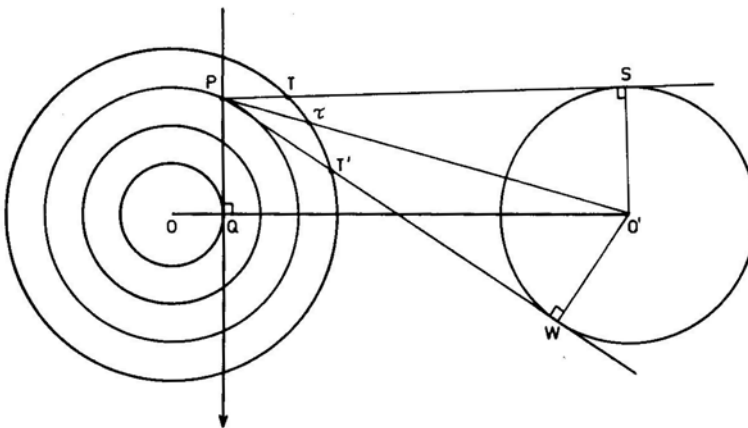
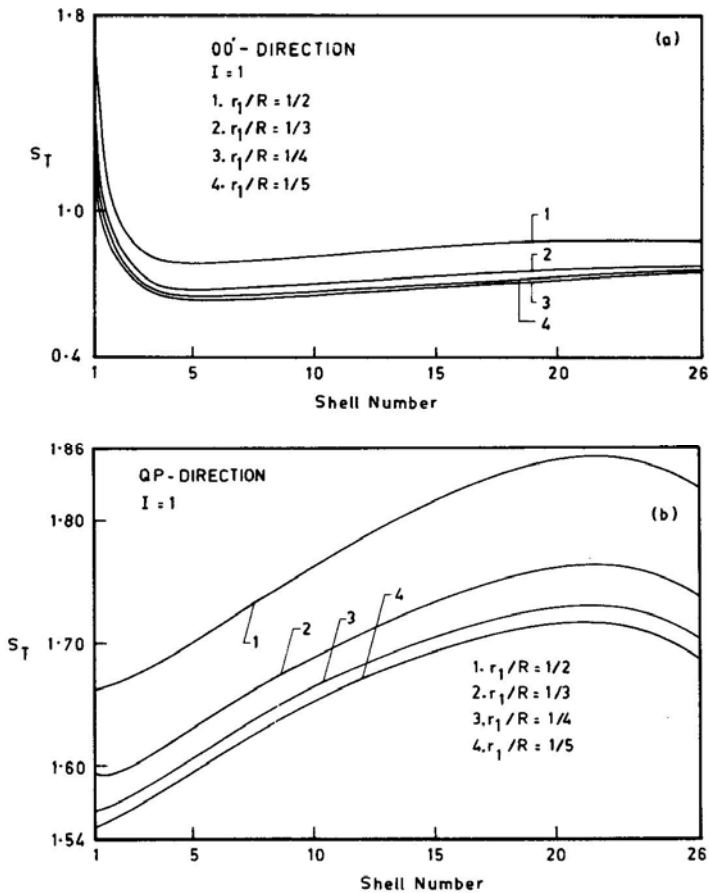


Figure 1. Schematic diagram of the model.

the shell boundaries. The total source functions  $S_T$  is given by

$$S_T = S_1 + S_s \tag{2}$$

The radius of the primary is taken to be  $10^{12}$  cm and the atmosphere is taken as half of the stellar radius. The primary and the secondary components are assumed to have equal radii. We have assumed an electron density of  $10^{13}$   $\text{cm}^{-3}$  at the innermost radius of the atmosphere and let it vary as  $1/r^2$ . The source function due to reflection changes considerably whether we go along  $OO'$  direction or along  $QP$  direction. The quantity  $S_s$  is the same along the boundary of a given shell because of spherical symmetry although this will be different for different shells. We have plotted the total source function with respect to the shell number. We have also studied the effect of proximity of the secondary component to the primary in terms of the parameter  $r_1/R$  where  $r_1$  is the radius of the primary and  $R = OO'$ . Another quantity we have used is  $I$ , the ratio of the luminosities of the primary and the secondary (see Paper 2). The total source function  $S_T$  is plotted in Figs 2 and 3. In Fig. 2(a),  $S_T$  is plotted for the  $OO'$  direction with  $I = 1$  and  $r_1/R = 1/2, 1/3, 1/4, 1/5$ . In all these figures, shell numbers 1 and 26



**Figure 2.** The total source function  $S_T$  corresponding to different shell numbers is plotted for  $I = 1$  along (a)  $OO'$  direction and (b)  $QP$  direction.  $S_T$  is given in arbitrary units.

correspond to the innermost and outermost radii of the atmosphere respectively. The source functions have their maxima at shell number 1 and fall rapidly before they reach shell number 4 where they reach the minimum values and then start to increase slowly towards shell number 25. The increase is not as fast as the fall at the innermost shells simply because the electron density falls as  $1/r^2$ ; as soon as the source function reaches a minimum value, the irradiation from the secondary takes over and the source function starts increasing. As the number density of electrons falls towards the outer radius, the amount of scattered radiation also falls. Therefore, the increase in the source function is not steep. The differences introduced into  $S_T$ , by the changes in the parameter  $r_1/R$  are not very large as can be seen from the figure. The curves corresponding to the last two cases (*i.e.*)  $r_1/R = 1/4$  and  $1/5$  merge together. In Fig. 2(b), we have plotted  $S_T$  with respect to shell number along the line of sight, *i.e.* along QP, where OQ is the innermost radius of the atmosphere. The behaviour of  $S_T$  along QP

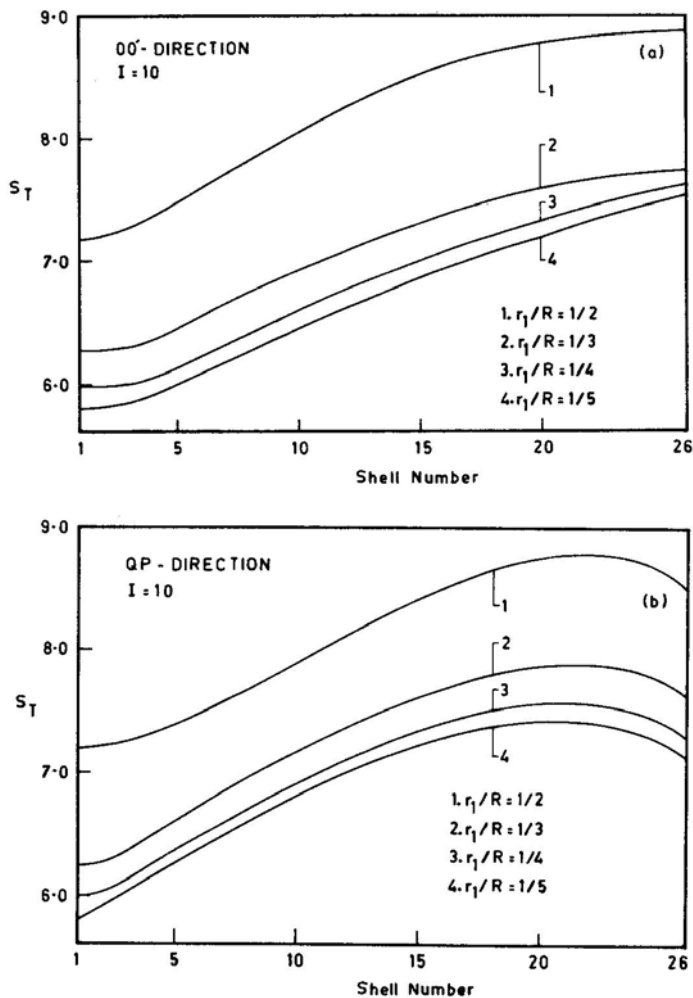


**Figure 3.** The total source function  $S_T$  corresponding to different shell numbers is plotted for  $I = 10$  along (a)  $OO'$  direction and (b)  $QP$  direction,  $S_T$  is given in arbitrary units.

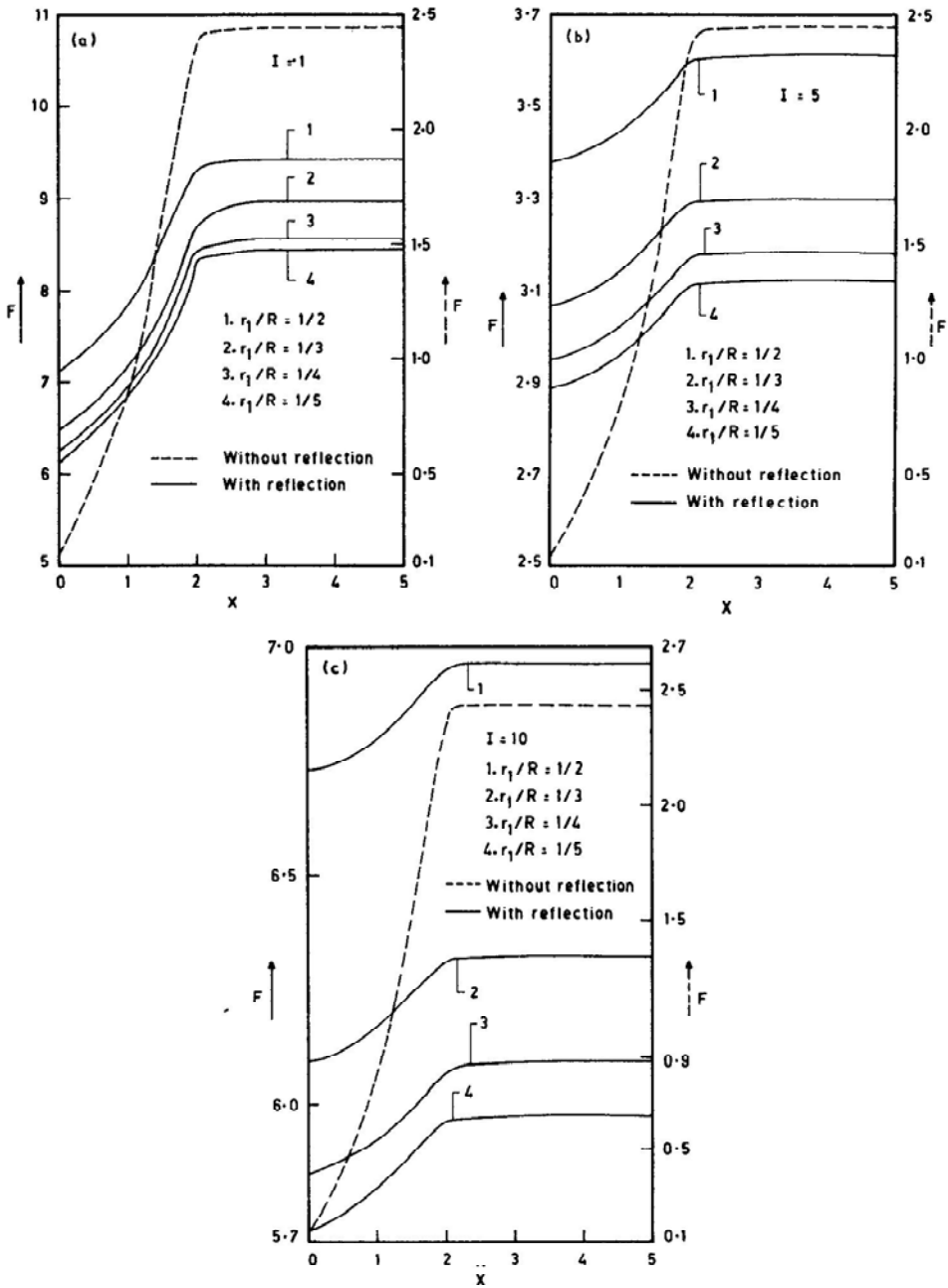


**Figure 4.** The flux profiles of lines are given in arbitrary units for (a)  $I = 1$ , (b)  $I = 5$  and (c)  $I = 10$ . The dashed line represents the flux profile without irradiation and its ordinate scale is given on the right-hand side. The continuous lines represent the flux profiles with irradiation, whose scale is given on the left-hand side.

direction is completely different from  $S_T$  along  $OO'$  direction. The source functions start increasing from the inner shells and the increase is quite high until they reach maxima at about shell number 20 or 21. Then they start falling although quite slowly. This can be understood from the fact that the points such as P are easily reached by the rays as the density of the electrons in these parts falls as  $1/r^2$  and the radiation will not be attenuated as much as it would be along the axis  $OO'$ . The slight fall in  $S_T$  in the outermost shells is due to the fact that the incident beam itself is diluted by the  $\cos \theta$  factor where  $\theta$  is the angle between the radius vector and the path of the ray.

In Fig. 3 (a), we have plotted  $S_T$  along  $OO'$  direction corresponding to an increased incident radiation ( $I = 10$ ). The results are quite different from those given in Fig. 2(a) for  $I = 1$ . The increased irradiation changes the variation of the source function. The quantity  $S_T$  along  $OO'$  in this case keeps on increasing although there is a gradual flattening towards the outer layers of the atmosphere. The source function along QP direction with the increased irradiation (Fig. 3b) behaves very similar to that given in Fig. 2(b), but with enhanced magnitude.

The flux profiles are plotted in Fig. 4 for  $I = 1, 5$  and  $10$ . We have considered a line with  $x = \pm 5$  Doppler units and employed a Doppler profile. When there is no irradiation, we obtain lines with deep cores. When irradiation is introduced the flux in the lines is increased considerably at all points in the line. But the increase in flux in the cores ( $F_c$ ) is considerably more than in the wings ( $F_w$ ). For example in Fig. 4(a), the ratio  $F_w/F_c$  is about 25 when there is no irradiation (the dotted curve). But in the presence of irradiation this ratio reduces to 1.3–1.4 depending on the proximity of the secondary. Because of irradiation, the flux in the whole line is dramatically increased disproportionately, the cores benefitting more than the wings. The same phenomenon occurs when the strength of the incident beam is increased as shown in Figs 4(b) and (c). The equivalent width has been calculated by using the formula

$$W = \int_{-x}^{+x} (1 - F_x/F) dx \quad (3)$$

where  $F$  and  $F_x$  are the fluxes in the continuum and at a frequency  $x$ .  $\alpha$  is the half band width of the line and is taken to be equal to 5 Doppler units. These equivalent widths are given in Table 1.

**Table 1.** The equivalent widths ( $W$ ) in Doppler units. Equivalent width without reflection = 2.34. Note how the enhanced irradiation reduces the equivalent widths.

| $I$ | $r_1/R$ | 1/2  | 1/3  | 1/4  | 1/5  |
|-----|---------|------|------|------|------|
| 1   |         | 0.61 | 0.65 | 0.67 | 0.68 |
| 5   |         | 0.16 | 0.17 | 0.18 | 0.18 |
| 10  |         | 0.08 | 0.09 | 0.10 | 0.10 |

In this paper, we have shown by a simple calculation, how the profiles of absorption lines change in a scattering medium with reflection. However, one should consider the temperature changes due to irradiation and also the effects of orbital revolution on the formation of spectral lines. This is under investigation.

**References**

- Grant, I. P., Peraiah, A. 1972, *Mon. Not. R. astr. Soc.*, **160**, 239.  
Napier, W. McD., Ovensen, M. W. 1970, *Astr. Astrophys.*, **4**, 129.  
Peraiah, A. 1982, *J. Astrophys. Astr.*, **3**, 485 (Paper 1).  
Peraiah, A. 1983a, *J. Astrophys. Astr.*, **4**, 11 (Paper 2).  
Peraiah, A. 1983b, *J. Astrophys. Astr.*, **4**, 151 (Paper 3).  
Peraiah, A., Rao, M. S. 1983, *J. Astrophys. Astr.*, **4**, 175 (Paper 4).  
Young, R. K. 1922, *Pub. Dominion Astrophys. Obs.*, **1**, 105.